DALTON
FULL PAPER

Kinetics and mechanism of the cobaloxime(II)-catalysed oxidative dehydrogenation of 3,5-di-*tert*-butylcatechol by O_2. A functional oxidase model

László I. Simándi * and Tatiana L. Simándi

Central Research Institute for Chemistry for the Hungarian Academy of Sciences, H-1525 Budapest, PO Box 17, Hungary

Received 13th May 1998, Accepted 28th July 1998

Triphenylphosphinecobaloxime(II) has been found to be a selective catalyst for the oxidative dehydrogenation of 3,5-di-*tert*-butylcatechol to the corresponding 1,2-benzoquinone at room temperature and atmospheric dioxygen pressure. In a rapid initial phase the catalyst is reversibly transformed to a previously characterised catecholato-cobaloxime(III) species, which persists throughout the reaction, keeping Co^{II} at a low level. The semiquinone anion radical ($dbsq^{\cdot -}$) and its cobaloxime(III) complex $Co^{III}(dbsq^{\cdot -})$ have been detected as intermediates by ESR spectroscopy. The kinetics was followed by volumetry. According to the proposed mechanism, in the rate-determining step superoxocobaloxime ($Co^{III}O_2$) abstracts an H atom from the cathechol *via* an hydrogen-bonded intermediate. The system investigated is a functional model of catecholase (oxidase) activity, based on free-radical intermediates, a possibility recently demonstrated for certain oxidoreductases.

The catalytic oxidation of catechols by transition metal complexes has been attracting interest because of its relevance to dioxygenase action. In combination with monooxygenases, dioxygenases play key roles in the metabolism of aromatic compounds. Catechol dioxygenases effect the intra- and extra-diol cleavage of catechol derivatives. Functional catechol dioxygenase models based on iron, copper and cobalt complexes have been designed and investigated with respect to their structure, kinetics and mechanisms.[1] The objective has been to elucidate mechanistic details and help understand how the enzyme active sites operate under biological conditions.

The diol cleavage reactions have been extensively studied [1a–e] using 3,5-di-*tert*-catechol (H_2dbcat) as a convenient model substrate. Iron complexes predominate among the functional models but other metals (Cu, Co, Mn, Ru, V) have also been used to elucidate mechanistic aspects. Cleavage of H_2dbcat is usually accompanied with oxidative dehydrogenation (catecholase activity) leading to the formation of 3,5-di-*tert*-butyl-1,2-benzoquinone (dtbq) in considerable yields.[1a–e] This type of oxidase activity is exhibited, *e.g.*, by tyrosinase and galactose oxidase. Relatively fewer studies have been carried out on the mechanism of this simple reaction using metal complexes as catalysts, although it may be a useful source of information on the mechanism of diol cleavage, owing to the possible presence of common intermediates. Most of these studies involved copper complexes.[2–13] An important point is the role of dioxygen complexes, which is not understood in sufficient detail. Cobalt complexes are known to bind dioxygen to form a variety of superoxo and peroxo species, which are involved in catalytic oxidations.[1d] They are therefore useful functional models for dioxygenase action. Oxidation of H_2dbcat by O_2 is catalysed by cobalt chelate complexes;[14–17] the system involving $[Co(acac)_2]$ has been investigated kinetically.[15,16] Although $[Co(acac)_2]$ does not form stable dioxygen complexes, the mechanisms proposed for dtbq formation from H_2dbcat involve a superoxocobalt intermediate, which may either generate a semiquinone anion radical by H-atom abstraction,[15] or simultaneously transfer two electrons to a co-ordinated catecholate.[16] The catalytic oxidation of semiquinones, possible intermediates in diol cleavage, has been studied in the presence of $[Co(acac)_2]$ and Co(salen) type complexes.[18] The superior activity of the former catalyst indicates that electron transfer, rather than dioxygen activation, is the step accelerated by the catalyst in this overall one-electron process.

The differing views on the roles dioxygen complexes may play in catechol oxidative dehydrogenation (catecholase activity) prompted us to carry out a kinetic study of a system in which (i) dioxygen complexes are formed, and (ii) intermediates for one- *vs.* two-electron processes can be distinguished with reasonable certainty.

We have previously reported that the cobaloxime(II) derivative $[Co(Hdmg)_2(Ph_3P)_2]$ is active in the selective catalytic conversion of H_2dbcat into dtbq with dioxygen at room temperature.[19] The blue complex $[Co(Hdmg)_2(Ph_3P)(Hdbcat)]$, containing a unidentate catecholate ligand in axial position, has been isolated from the reaction mixture and characterised by X-ray diffraction. The ESR studies have revealed the involvement of the free 3,5-$dbsq^{\cdot -}$ semiquinone anion radical and the complex $[Co(Hdmg)_2(Ph_3P)(dbsq^{\cdot -})]$ as intermediates.[19]

In this paper we report volumetric, spectrophotometric and HPLC studies aimed at elucidating the kinetics and mechanism of the cobaloxime-catalysed oxidation of H_2dbcat. In the absence of catalyst no oxidation can be detected under the same conditions.

Experimental

The complex $[Co(Hdmg)_2(Ph_3P)_2]$ was synthesized by the procedure reported; H_2dbcat was an Aldrich product.

The catalytic reaction was carried out in methanol solution. Monitoring was done by gas volumetry, spectrophotometry and HPLC. At O_2 pressures greater than 1 bar, a Parr pressure vessel equipped with a magnetic stirrer was used.

Rates of dioxygen uptake were measured in a constant pressure gas-volumetric apparatus. To start the reaction the solid cobaloxime(II) catalyst was added to a vigorously stirred, thermally equilibrated methanol solution of the H_2dbcat substrate from a sample holder manipulated from the outside. The volume of absorbed O_2 was read periodically using a gas burette. The rate of absorption was independent of the stirring rate, excluding eventual diffusion control effects.

The kinetics of oxidation was also followed by recording the

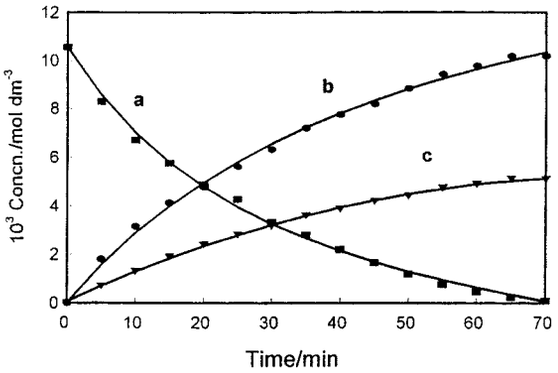

Fig. 1 Formation of dtbq by the cobaloxime(II)-catalysed oxidation of H_2dbcat as monitored by HPLC and gas volumetry. Solvent MeOH, $[Co]_0 = 0.568 \times 10^{-3}$, $[H_2dbcat]_0 = 1.03 \times 10^{-3}$, $[O_2] = 1.1 \times 10^{-3}$ mol dm^{-3}. (a) H_2dbcat, (b) dtbq, (c) dioxygen uptake.

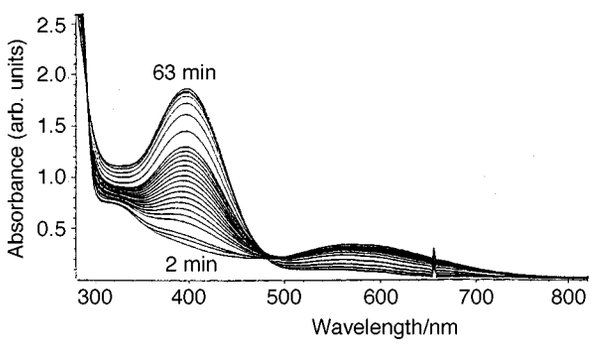

Fig. 2 Time evolution of spectra during the cobaloxime(II)-catalysed oxidation of H_2dbcat in MeOH under pure O_2 ($l = 1$ cm). $[Co(Hdmg)_2(Ph_3P)_2]_0 = 0.613 \times 10^{-3}$, $[H_2dbcat]_0 = 9.26 \times 10^{-3}$, $[O_2] = 1.1 \times 10^{-3}$ mol dm^{-3}.

successive UV/VIS spectra on a Hewlett-Packard 8452A diode array spectrophotometer. Infrared spectra in KBr pellets were recorded on a Specord 75 spectrometer, ESR spectra on a JES-FE-3X spectrometer (X-band, operating frequency 9.5 GHz).

The HPLC analyses were performed on a Waters 991 system with a diode array detector [silica column Spherisorb 5 μm, eluent methanol–water (80:10); elution rate 1.0 cm^3 min^{-1}]; detection of dtbq at 280 nm ($R_t = 6.8$ min), H_2dbcat at 280 nm ($R_t = 8.4$ min). Calibration with four or five samples of different masses was reproducible within about 1%. Samples withdrawn from the reacting mixture for HPLC analysis were quenched by 11-fold dilution with MeOH before injection.

Results and discussion

Stoichiometry

According to parallel gas-volumetric and HPLC measurements, the stoichiometry of oxidation corresponds to eqn. (1). Fig. 1

$$H_2dbcat + 0.5O_2 \longrightarrow dtbq + H_2O \qquad (1)$$

shows typical concentration *vs.* time curves for H_2dbcat and dtbq obtained by HPLC. The mass balance required by eqn. (1) is fulfilled within ±2%. No other oxidation products can be detected by HPLC or TLC.

Intermediates

Spectrophotometry. The catalytic reaction was also monitored by spectrophotometry after injecting a cobaloxime(II) solution prepared under N_2 into an O_2-saturated solution of H_2dbcat in MeOH. Stirring of the mixture under air or O_2 was interrupted only for recording the spectra at intervals. The time

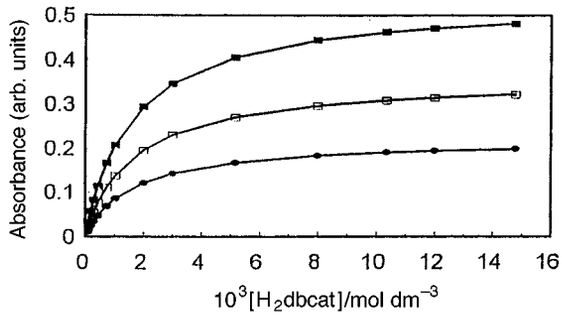

Fig. 3 Initial absorbance jumps at 570 nm at various cobaloxime(II) and H_2dbcat concentrations, taken from the spectra recorded 30 s after preparing the solution (25 °C, MeOH). $[Co]_0$ (●) 0.616×10^{-3}, (□) 1.0×10^{-3}, (■) 1.50×10^{-3} mol dm^{-3}.

evolution of the spectrum is shown in Fig. 2. The most prominent feature of the spectral changes is that a dark blue complex with a wide band centred at 570 nm appears immediately (within about 2–30 s) after mixing the colourless H_2dbcat and the pale yellow cobaloxime(II) solution. The initial absorbance jump suggests that a significant part of the added $[Co(Hdmg)_2(Ph_3P)_2]$ is rapidly converted into the strongly coloured $[Co(Hdmg)_2(Ph_3P)(Hdbcat)]$, which thereafter is a major cobaloxime species in the reacting system, persisting at an approximately constant level.

In the ensuing steady state, which lasts for about 15–20 min, the solution is absorbing dioxygen and H_2dbcat is being converted into dtbq ($\lambda = 400$ nm). During this process the spectra exhibit an isosbestic point at 495 nm. There is excellent agreement between the amounts of dtbq calculated from the volumetric curves, the absorbance at 400 nm and also HPLC analysis. At later stages (25–63 min) the 570 nm band decreases.

We have measured the initial absorbance jump (after 30 s), equal to the steady-state absorbance at 570 nm (persisting for over 15–20 min), as a function of the starting H_2dbcat and $[Co(Hdmg)_2(Ph_3P)_2]$ concentrations. The results are shown in Fig. 3. At constant cobaloxime concentration an increasing excess of H_2dbcat leads to saturation type curves, indicating an increasing extent of formation of the coloured complex. The ratio of $A : A_{sat}$ (where A_{sat} is the estimated saturation value of the absorbance at 570 nm) is on the average equal to $0.84 \pm 0.04 : 1$. Also the value of A at sufficiently high catechol to cobaloxime ratio (*ca.* 10:1 or higher), approximately equal to A_{sat}, is proportional to the cobaloxime concentration, providing a molar absorptivity of $\varepsilon = 7140$ dm^3 mol^{-1} cm^{-1} for the coloured species.

These results will be utilised in the kinetic measurements for estimating the relative concentration of free cobaloxime(II) in the steady state. It should be generally much lower than the overall value corresponding to the added amount, because otherwise the oxygenation rate would be too large to measure. [The oxygenation of cobaloxime(II) occurs on the stopped-flow timescale at the concentration levels used in this work.[21]] Further kinetic implications of these results with respect to the kinetic behaviour will be discussed in the section on kinetics.

ESR spectroscopy

The reaction was also monitored by ESR spectroscopy under the same conditions as the successive UV/VIS spectra were recorded. The complex $[Co(Hdmg)_2(Ph_3P)_2]$ was added to a stirred MeOH solution of H_2dbcat under air. Samples were withdrawn at intervals and transferred to ESR tubes. The observed behaviour was the same as that reported previously, so only a brief account is given of these data. The first spectrum was recorded *ca.* 2 min after mixing the reactants. It consisted of an eight-line signal with $g = 2.0017$ and $A_{Co} = 10.4$ G, which persisted throughout the period the reaction was followed (30–

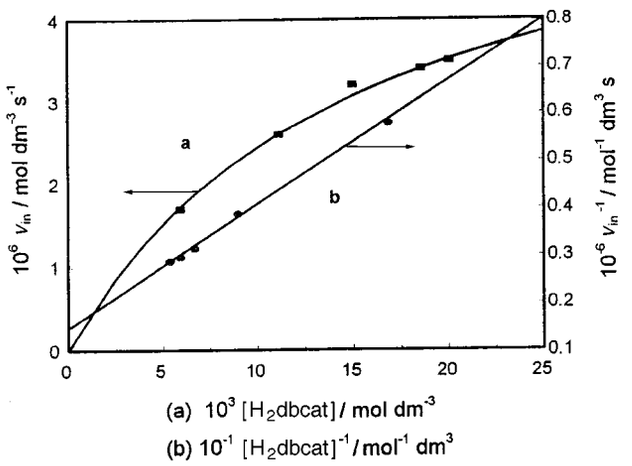

Fig. 4 (a) Dependence of the initial rate of dioxygen uptake on the concentration $[H_2dbcat]_0$ in MeOH; $[Co(Hdmg)_2(Ph_3P)_2]_0 = 1.0 \times 10^{-3}$, $[O_2] = 1.0 \times 10^{-3}$ mol dm^{-3}. (b) Plot of $1/v_{in}$ *vs.* $1/[H_2dbcat]_0$.

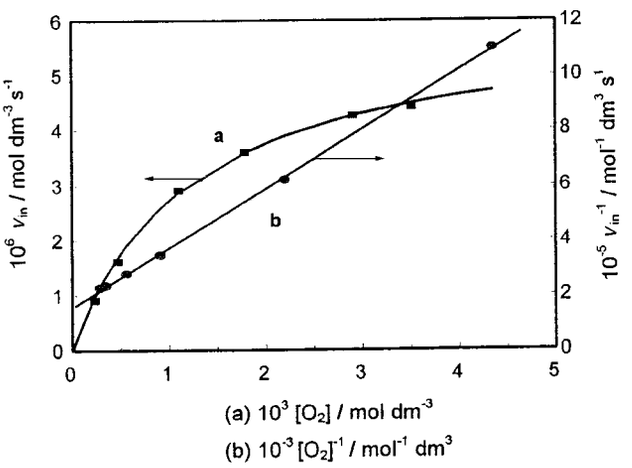

Fig. 5 (a) Dependence of the initial rate of dioxygen uptake on the dioxygen concentration in MeOH, $[Co(Hdmg)_2(Ph_3P)_2]_0 = 1.0 \times 10^{-3}$, $[H_2dbcat]_0 = 1.5 \times 10^{-2}$ mol dm^{-3}. (b) Plot of $1/v_{in}$ *vs.* $1/[O_2]$.

40 min). Each line was a doublet with a coupling constant of 3.3 G. At higher resolution an 18-line signal was observed at the centre of the eight-line signal ($g = 2.0046$, $A_{2H} = 1.7$, $A_{18H} = 0.35$ G). These signals are identical to those reported earlier for the cobaloxime(II)–H_2dbcat–O_2 system.[19] The eight-line signal is consistent with the formation of a cobaloxime(III) derivative containing a unidentate 3,5-di-*tert*-butyl-1,2-benzosemiquinonato(1−) anion radical (dbsq$^{\bullet -}$) as axial ligand, [$Co^{III}(Hdmg)_2(Ph_3P)$(dbsq$^{\bullet -}$)]. The 18-line signal corresponds to free dbsq$^{\bullet -}$. It is remarkable that the wide spectral band with $\lambda_{max} = 730$ nm ($\varepsilon = 680$ dm^3 mol^{-1} cm^{-1}) reported for the dbsq$^{\bullet -}$ anion radical[18,22,23] could not be detected, probably because of its low intensity.

Kinetic measurements

The time dependence of dioxygen absorption was measured by gas volumetry in methanol as solvent. Initial rates of dioxygen-uptake (v_{in}) were determined in the persisting steady state reached after mixing the reactants, *i.e.* when the solution turned blue and had a steady absorbance for an extended period of time (see Fig. 2). These data were used for deducing the kinetic equation. The initial rate (v_{in}) was found to be proportional to the catalyst concentration, implying a first order dependence. The dependencies of v_{in} on the substrate and dioxygen concentration are shown in Figs. 4 and 5. Each point corresponds to the average of two or three individual runs reproducible to within ±5%. There is a first order dependence on the cobaloxime concentration, but saturation type kinetics are observed for the dependencies of the initial rate on both the H_2dbcat and dioxygen concentration. The corresponding plots of $1/v_{in}$ against $1/[H_2dbcat]_0$ and $1/[O_2]$ are linear, as is shown by Figs. 4 and 5, respectively.

The observed kinetic behaviour is consistent with the reaction mechanisms in eqns. (2)–(5), and (7)–(10), where Co^{II} and Co^{III} represent the [$Co^{II}(Hdmg)_2(Ph_3P)$] and [$Co^{III}(Hdmg)_2(Ph_3P)$]$^+$ moiety, respectively. {Upon dissolution [$Co(Hdmg)_2(Ph_3P)_2$] is known to lose one of the axial Ph_3P ligands.[24]} Earlier kinetic work has revealed that the oxygenation of cobaloxime(II) in MeOH is very fast, taking place on the stopped-flow timescale.[21]

In the fast pre-steady state reaction, taking less than about 30 s, all of the cobaloxime(II) added initially is first reversibly oxygenated to the superoxo species $Co^{III}O_2$ and then converted into the blue complex Co^{III}(Hdbcat) characterised earlier. These rapid reactions occur *via* the sequence of steps (2)–(5), corresponding to the overall reaction (6). According to this

$$Co^{II} + O_2 \overset{K_1}{\rightleftharpoons} Co^{III}O_2 \quad (2)$$

$$Co^{III}O_2 + H_2dbcat \overset{K_2}{\rightleftharpoons} \mathbf{X} \quad (3)$$

$$\mathbf{X} \xrightarrow{k_3} Co^{III}O_2H + dbsq^{\bullet -} + H^+ \quad (4)$$

$$Co^{II} + dbsq^{\bullet -} + H^+ \rightleftharpoons Co^{III}(Hdbcat) \quad (5)$$

$$2Co^{II} + O_2 + H_2dbcat \xrightarrow{\text{fast}} Co^{III}(Hdbcat) + Co^{III}O_2H \quad (6)$$

scheme, cobaloxime(II) is first oxygenated to superoxocobaloxime, which forms a hydrogen-bonded intermediate **X** with H_2dbcat in a reversible step. This is followed by H-atom abstraction, producing the semiquinonato(1−) anion radical dbsq$^{\bullet -}$, which combines with the paramagnetic cobaloxime(II), affording the intermediate Co^{III}(Hdbcat), which has been isolated and characterised. Intermediate **X** is required by the rate law indicating pre-equilibria of the cobaloxime(II) catalyst with both the substrate and O_2.

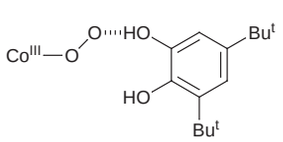

X

In the steady state following the fast initial phase the overall stoichiometry (1) requires that O_2 be reduced to H_2O, rather than H_2O_2, therefore the hydroperoxocobaloxime $Co^{III}O_2H$ formed in step (4) should undergo disproportionation, regenerating one half of the O_2 absorbed and producing the hydroxocobaloxime $Co^{III}OH$ (step 7). Also, for a sustained catalytic

$$2Co^{III}O_2H \longrightarrow 2Co^{III}OH + O_2 \quad (7)$$

$$Co^{III}OH + dbsq^{\bullet -} + H^+ \longrightarrow Co^{II} + dtbq + H_2O \quad (8)$$

$$Co^{III}OH + Co^{III}(Hdbcat) \longrightarrow Co^{II} + Co^{III}(dbsq^{\bullet -}) + H_2O \quad (9)$$

$$Co^{III}(dbsq^{\bullet -}) \rightleftharpoons Co^{II} + dtbq \quad (10)$$

cycle to occur in the steady state, a route to the product dtbq and a path regenerating the cobalt(II) catalyst are necessary. These requirements of a catalytic cycle are fulfilled by addition

of electron transfer steps (8) and (9) to the mechanism. Formation of the cobaloxime derivative $Co^{III}(dbsq^{\cdot -})$ exhibiting the eight-line ESR signal observed during the catalytic oxidation can be explained by reaction (9). It is also involved in equilibrium (10), which has been demonstrated by treating cobaloxime(II) with dtbq under N_2, when the same ESR spectrum was obtained.

A remarkable feature of the mechanism in eqns. (2)–(10) is that the dioxygen activation steps (2) and (3) are involved in both the rapid initial phase and also the steady state. They control the rate of dioxygen uptake by the reacting solution, which, however, differs very strongly in these two phases. This implies that as the system reaches the steady state very shortly after mixing the reactants the concentration of Co^{II} drops to a fraction of the starting value, so that the dioxygen consumption rate falls from the stopped-flow level[21] to values susceptible to monitoring by gas volumetry.

The steady state kinetic equation for the oxidation of H_2dbcat can be derived on the following assumptions: (i) the cobaloxime(II) reactive towards O_2 is in fast equilibrium with both the superoxo and the Co^{III}(Hdbcat) species; (ii) O_2 enters the cycle *via* steps (2)–(4), one half of it being released in step (7); (iii) the rate-determining step is (4), whereas (2) and (3) are fast pre-equilibria; (iv) the combination step (5) is fast.

The mass balance for the cobaloxime species is given by eqn. (11) where $[Co]_0 = [Co(Hdmg)_2(Ph_3P)_2]_0$. At the early stages

$$[Co]_0 = [Co^{II}] + [Co^{III}O_2] + [X] + [Co^{III}O_2H] + [Co^{III}(Hdbcat)] + [Co^{III}OH] + [Co^{III}(dbsq^{\cdot -})] \quad (11)$$

after the steady state is reached, *i.e.* where the initial rates v_{in} are measured, the concentration of dtbq is negligible, therefore, reaction (10) and the amount of its product can be neglected, *i.e.* $[Co^{III}(dbsq^{\cdot -})] \approx 0$. Also, the large excess of H_2dbcat rapidly converts CoO_2 into **X**, so the concentration of CoO_2 is negligible, $[Co^{III}O_2] \approx 0$. (The same conclusion has been reached from the treatment of kinetic data, see below).

According to the stoichiometry of the rapid phase [eqn. (6)], Co^{III}(Hdbcat) and $Co^{III}O_2H$ are formed in equal amounts, which is expressed by eqn. (12). The above considerations lead

$$[Co^{III}(Hdbcat)] \approx [Co^{III}O_2H] \quad (12)$$

to the simplified balance equation (13). The rate of O_2 uptake

$$[Co]_0 \approx [Co^{II}] + [X] + [Co^{III}(Hdbcat)] + [Co^{III}O_2H] \quad (13)$$

is given by eqn. (14) where the concentration of **X** on the

$$v_{in} = k_3[X] = k_3K_1K_2[O_2][H_2dbcat][Co^{II}] \quad (14)$$

right-hand side is written in terms of the equilibrium constants of (2) and (3) and the appropriate concentrations. In eqn. (14) the dioxygen concentration is to a good approximation equal to that of the saturated solution, because intense stirring of the reacting solution eliminates diffusion effects. Also, the concentration of H_2dbcat can be replaced by its initial value at low conversions into the product.

The concentration of free cobaloxime(II) can be expressed from eqn. (13) using the equilibrium constants K_1 and K_2 [eqn. (15)]. Substitution of $[Co^{II}]$ into eqn. (14) yields kinetic equation

$$[Co^{II}] = \frac{[Co]_0 - 2\,[Co^{III}(Hdbcat)]}{1 + K_1K_2[O_2][H_2dbcat]_0} \quad (15)$$

(16) for the rate of dioxygen absorption. The difference in the

$$v_{in} = k_3[Co^{II}] \approx k_3\frac{K_1K_2[O_2][H_2dbcat]_0\{[Co]_0 - 2\,[Co^{III}(Hdbcat)]\}}{1 + K_1K_2[O_2][H_2dbcat]_0} \quad (16)$$

Table 1 Summary of rate and equilibrium constants from eqn. (18).

			Slope/s^{-1}	
Source	k_3/s^{-1}	$K_1K_2/dm^6\ mol^{-2}$	exptl.	calc.
Fig. 5	3.73×10^{-2}	5.43×10^4		
Fig. 6	3.94×10^{-2}	4.87×10^4		
Fig. 4			2.14×10^{-3}	2.37×10^{-3}

numerator of eqn. (15) can be expressed using the spectrophotometric results shown in Fig. 3 and eqn. (12). At the $[H_2dbcat]_0$ to $[Co]_0$ ratios employed in the kinetic measurements ($R > 7$), the approximate equality (17) is valid, which, upon

$$A/A_{sat} \approx \varepsilon[Co^{III}(Hdbcat)]/0.5\varepsilon[Co]_0 \approx 0.84 \pm 0.04 \quad (17)$$

$$v_{in} = k_3\frac{0.16\,K_1K_2[O_2][H_2dbcat]_0[Co]_0}{1 + K_1K_2[O_2][H_2dbcat]_0} \quad (18)$$

substitution into eqn. (16), yields the final form (18) of the kinetic equation (A_{sat} is the saturation value of absorbance in Fig. 3 and ε the molar absorbance of the coloured complex). Eqn. (18) is consistent with the double reciprocal plots shown in Figs. 5 and 6. It should be noted that if $[CoO_2]$ were not neglected, an additive $K_1[O_2]$ term would appear in the denominator of eqn. (18). However, calculations using that expression, which also leads to linear reciprocal plots, yield a negative value for K_1, therefore an alternative interpretation is needed. The assumption that in the denominator $K_1[O_2]$ is negligible compared with the other two terms leads to positive and consistent values listed in Table 1.

The mechanism consisting of steps (2)–(10) describes the behaviour of a catecholase model which affords the *o*-quinone as the sole oxidation product without any ring cleavage reactions. The reasons for this selectivity merit consideration. In catechol dioxygenases and model systems based on iron complexes *o*-quinone formation is often observed beside cleavage products. Ring cleavage with oxygen incorporation requires that dioxygen be attached to a carbon-centred radical in the catechol ring, forming a peroxy species, which can be rearranged to the observed muconic anhydride or carboxyhydroxymethylfuran product *via* ring expansion or contraction,[1b,e] respectively. For this process to occur the catechol should first be converted into the semiquinone anion radical, the carbon-centred forms of which may bind O_2 *via* two pathways: (i) direct attack by free O_2, or (ii) attack by a metal-bound superoxide ligand. The semiquinone may in turn be free or co-ordinated to the metal. This is a mechanistic feature of major importance, which has not yet been fully resolved, although arguments have been put forward for both possibilities.[1a–e,17,18]

The present system does not allow the adjacent co-ordination of a catecholate and a superoxide ligand owing to the very stable equatorial $(Hdmg)_2$ macrocycle, which is the reason why no ring cleavage products are observed. In principle, it would also be possible for unco-ordinated $dbsq^{\cdot -}$ to react with O_2 to produce a carbon-centred peroxy radical, which could generate cleavage products, as has been observed by White and Que[18] in the $[Co(acac)_2]$ catalysed oxidation of 3,5-di-*tert*-butyl-*o*-benzosemiquinone. Obviously, in the cobaloxime system, this cleavage path is kinetically not favourable due to the low level of $dbsq^{\cdot -}$ concentration caused by equilibrium (5) being shifted to the right and the rapidity of electron transfer step (8), steering the oxidation exclusively to dtbq formation.

The role of dioxygen complex formation [eqn. (2)] is of fundamental importance in the cobaloxime(II) system, which upon exposure to O_2 is rapidly converted into superoxo and peroxo species, and ultimately to cobaloxime(III).[21] The catalytic activity is due to the transient superoxo complex[25–27] and the

continuous regeneration of the cobaloxime(II) species [eqns. (7) and (8)]. Cobaloxime(III) is catalytically inactive in oxidations but over extended periods reducing substrates may slowly generate cobaloxime(II), which then exhibits catalytic activity.

In the $[Co(acac)_2]$-catalysed oxidation of H_2dbcat a superoxo complex has been proposed as the active oxidant[15,16] although its instability has thus far precluded detection and/or isolation. The present work provides further support to the key role of dioxygen complexes in oxidative dehydrogenations catalysed by metal complexes, which may be regarded as functional models for oxidases with catecholase activity.

The involvement of free radical intermediates calls attention to similarity to the celebrated cases of free-radical mechanisms in oxidoreductases like galactose oxidase and ribonucleotide reductase.[28] The oxidised active site of galactose oxidase contains a single copper(II) ion and a co-ordinated tyrosyl radical, which together represent the two oxidation equivalents required for the transformation of RCH_2OH type substrates to RCHO. Reoxidation of the reduced active site consisting of Cu^{I} and co-ordinated tyrosine is brought about by dioxygen. In the caboloxime–H_2dbcat system an analogous active site model is the $Co^{III}(dbsq^{\cdot -})$ complex, detected by ESR spectroscopy, which is a cobaloxime(II)-bound semiquinone anion radical. It is capable of releasing the oxidation product dtbq and the reduced catalyst Co^{II} [eqn. (10)], which then returns into the cycle. In our case the free-radical type ligand is derived from the substrate to be oxidised, but otherwise the similarity is remarkable. Work is in progress on the design and elucidation of other functional oxidase active site models.

$$\underset{\text{catalyst}}{Co^{II}} + \underset{\substack{\text{substrate (reduced}\\ \text{free radical)}}}{H_2\text{dbcat}} + 0.5\,O_2 \longrightarrow \underset{\text{active site}}{Co^{III}(dbsq^{\cdot -})} + H_2O \qquad (19)$$

$$\underset{\text{active site}}{Co^{III}(dbsq^{\cdot -})} \longrightarrow \underset{\text{catalyst}}{Co^{II}} + \underset{\text{product}}{\text{dtbq}} \qquad (20)$$

Acknowledgements

This work was supported by the Hungarian Research Fund (Grant T 015830) and by COST Chemistry Action D1 (PECO 12984).

References

1 (*a*) L. Que, jun., *Coord. Chem. Rev.*, 1983, **50**, 73; (*b*) L. Que, jun., in *Bioinorganic Catalysis*, ed. J. Reedijk, Marcel Dekker, New York, 1993, pp. 347–393; (*c*) C. G. Pierpont and C. W. Lange, *Prog. Inorg. Chem.*, 1994, **41**, 331; (*d*) L. I. Simándi, *Catalytic Activation of Dioxygen by Metal Complexes*, Kluwer, Dordrecht, Boston, London, 1992, ch. 6; (*e*) T. Funabiki, in *Oxygenases and Model Systems*, ed. T. Funabiki, Kluwer, Dordrecht, Boston, London, 1997, pp. 19–156; (*f*) A. Nishinaga, in *Oxygenases and Model Systems*, ed. T. Funabiki, Kluwer, Dordrecht, Boston, London, 1997, pp. 157–194.
2 L. K. Thompson and A. B. P. Lever, *Can. J. Chem.*, 1969, **47**, 4141.
3 A. B. P. Lever, B. S. Ramaswamy and S. R. Pickens, *Inorg. Chim. Acta*, 1980, **46**, L59.
4 N. Oishi, Y. Nishida, K. Ida and S. Kida, *Bull. Chem. Soc. Jpn.*, 1980, **53**, 2847.
5 D. Bolus and G. S. Vigee, *Inorg. Chim. Acta*, 1982, **67**, 19.
6 K. Moore and G. S. Vigee, *Inorg. Chim. Acta*, 1982, **66**, 125.
7 U. Casellato, D. Fregona, S. Sitran, S. Tamburini, P. A. Vigato and P. Zanello, *Inorg. Chim. Acta*, 1984, **95**, 279.
8 S. Tsuruya, H. Kuwahara and M. Masai, *J. Catal.*, 1987, **108**, 369.
9 S. Harmalker, S. E. Jones and D. T. Sawyer, *Inorg. Chem.*, 1983, **22**, 2790.
10 M. D. Stallings, M. M. Morrison and D. T. Sawyer, *Inorg. Chem.*, 1981, **20**, 2655.
11 R. M. Buchanan, C. Wilson-Blumenberg, C. Trapp, S. C. Larsen, D. L. Green and C. G. Pierpont, *Inorg. Chem.*, 1986, **25**, 3070.
12 É. Balogh-Hergovich and G. Speier, *Inorg. Chim. Acta*, 1985, **108**, 59.
13 M. R. Malachowski, B. Dorsey, J. G. Sackett, R. S. Kelly, A. L. Ferko and R. N. Hardin, *Inorg. Chim. Acta*, 1996, **249**, 85.
14 C. A. Tyson and A. E. Martell, *J. Am. Chem. Soc.*, 1972, **94**, 939.
15 H. Sakamoto, T. Funabiki, S. Yoshida and K. Tarama, *Bull. Chem. Soc. Jpn.*, 1979, **52**, 2760.
16 S. Tsuruya, S.-I. Yanai and M. Masai, *Inorg. Chem.*, 1986, **25**, 141.
17 S. Nakashima, H. Ohya-Nishiguchi, N. Hirota, S. Tsuboyama and T. Chijimatsu, *Stud. Surf. Sci. Catal.*, 1991, **66**, 347.
18 L. S. White and L. Que, jun., *J. Mol. Catal.*, 1985, **33**, 139.
19 L. I. Simándi, T. Barna, Gy. Argay and T. L. Simándi, *Inorg. Chem.*, 1995, **34**, 6337.
20 G. N. Schrauzer and L. P. Lee, *J. Am. Chem. Soc.*, 1970, **92**, 1551.
21 L. I. Simándi, C. R. Savage, Z. A. Schelly and S. Németh, *Inorg. Chem.*, 1982, **21**, 2765.
22 L. S. White, E. J. Hellman and L. Que, jun., *J. Org. Chem.*, 1982, **47**, 3766.
23 S. Muto and T. C. Bruice, *J. Am. Chem. Soc.*, 1980, **102**, 4472.
24 P. W. Schneider, P. F. Phelan and J. Halpern, *J. Am. Chem. Soc.*, 1969, **91**, 77.
25 L. I. Simándi, T. Barna, L. Korecz and A. Rockenbauer, *Tetrahedron Lett.*, 1993, **34**, 717.
26 L. I. Simándi, T. Barna and S. Németh, *J. Chem. Soc.*, *Dalton Trans.*, 1996, 473.
27 L. I. Simándi and T. L. Simándi, *J. Mol. Catal. A: Chemical*, 1997, **117**, 299.
28 E.-I. Ochiai, in *Metal Ions in Biological Systems*, eds. H. Sigel and A. Sigel, Marcel Dekker, New York, Basel, 1994, vol. 30, pp. 1–24; J. W. Whittaker, *Metal Ions in Biological Systems*, eds. H. Sigel and A. Sigel, Marcel Dekker, New York, Basel, 1994, vol. 30, pp. 315–403; K.-Y. Lam, D. G. Fortier and A. G. Sykes, *J. Chem. Soc.*, *Chem. Commun.*, 1990, 1019; K. D. Karlin, Z. Tyeklár and A. D. Zuberbühler, in *Bioinorganic Catalysis*, ed. J. Reedijk, Marcel Dekker, New York, 1993, pp. 261–315.

Paper 8/03597K